An Indoor Experiment in Decentralized Coordinated Search

Frédéric Bourgault, George Mathews, Alex Brooks, and Hugh F. Durrant-Whyte

ARC Centre of Excellence for Autonomous Systems (CAS)
Australian Centre for Field Robotics
The University of Sydney, Sydney, NSW 2006, Australia
{f.bourgault, g.mathews, a.brooks, hugh}@acfr.usyd.edu.au
http://www.acfr.usyd.edu.au

Abstract. This paper addresses the problem of coordinating a team of multiple heterogeneous sensing platforms searching for a single mobile target in a dynamic environment. The proposed implementation of an active sensor network architecture combines a general decentralized Bayesian filtering algorithm with a decentralized coordinated control strategy. In this approach, by communicating with their neighbors on the network, each decision maker builds an equivalent representation of the probability density function of the target state on which they base their control decision.

1 Introduction

Search and Rescue (SAR) is a forthcoming domain of application in field robotics. Interconnecting multiple autonomous search platforms into a network to share information and collaborate has the potential to increase the efficiency and the rate of success of such time critical missions where human life is at stake.

This paper addresses the problem of coordinating the search effort of an arbitrary number of decentralized sensing platforms. It presents an indoor implementation of the active Bayesian sensor network approach discussed in [1]. The approach combines a general decentralized Bayesian filtering technique with point-to-point communication and a decentralized coordinated control scheme. By adaptively exchanging information with their network neighbors, each sensor node builds an equivalent estimate of the Probability Density Function (PDF) of the target state on which they base their local control decisions. The information is transmitted between the nodes via managed channel filters guaranteeing the robust recovery of the complete global information at each node provided that the network connectivity is acyclic, i.e. tree-connected without loops. By mutually contributing to their PDF estimates, the decision makers influence each other, rendering their trajectories globally consistent and coordinated [3,9]. The resulting coordinated search trajectories explicitly consider the search vehicles kinematics, the arbitrary detection function of the sensors and the target motion model. The advantage of this modular approach is that a high degree of scalability and real time adaptability can be achieved.

The decentralized coordinated search framework was first explored in [3] where faultless broadcasted communication was assumed. The idea of integrating external motion constraints such as walls into the prediction stage was presented in [2]. A different search framework using Bayesian ideas can be found in [7] while [15] uses game theory combined with heuristics to find evading targets.

The paper is organized as follows. Sec. 2 reviews the decentralized Bayesian filtering algorithm and the decentralized coordinated control strategy implemented

M.H. Ang and O. Khatib (Eds.): Experimental Robotics IX, STAR 21, pp. 407–416, 2006.

in the architecture. Sec. 3 describes the searching problem. Then, Sec. 4 discusses the implementation details of the framework for a team of Pioneer robots searching for a person in a cluttered indoor environment and presents experimental search results. Finally, conclusions and ongoing research directions are highlighted.

2 Architecture

This section describes the framework for coordinating the search effort of a robotic team based on an Active Sensor Network (ASN) architecture [11]. ASN combines decentralized data fusion and decentralized control into a coherent architecture.

2.1 Decentralized Bayesian Filtering

In the searching problem, the unknown variable of interest is the target state vector at time step k, denoted $\mathbf{x}_k^t \in \mathbb{R}^{n_x}$, which in general describes the target location but could also include its attitude, velocity, and other properties. In this paper the superscripts t and s_i indicate a relationship to the target and the sensor i respectively. The subscripts are used to indicate the time index. The purpose of the analysis is to find an estimate for $p(\mathbf{x}_k^t|\mathbf{z}_{1:k})$, the PDF over $\mathbf{x}_k^t$ given the sequence $\mathbf{z}_{1:k} = \{\mathbf{z}_j^i : i = 1, ..., N_s, j = 1, ..., k\}$ of all the observations made from the N_s sensors on board the search vehicles, $\mathbf{z}_j^i$ being the observation from the i^{th} sensor at time step j. The analysis starts by determining a prior PDF $p(\mathbf{x}_0^t|\mathbf{z}_0) \equiv p(\mathbf{x}_0^t)$ for the target state at time 0, given all available prior information including past experience and domain knowledge. If nothing is known other than initial bounds on the target state vector, then a least informative uniform PDF is used as the prior. Once the prior distribution has been established, the PDF at time step k, $p(\mathbf{x}_k^t|\mathbf{z}_{1:k})$, can be constructed recursively using the prediction and update equations alternatively.

Prediction Suppose the system is at time step $k-1$ and the latest PDF update, $p(\mathbf{x}_{k-1}^t|\mathbf{z}_{1:k-1})$, is available. Then the predicted PDF of the target state at time step k is obtained from the following Chapman-Kolmogorov equation

$$p(\mathbf{x}_k^t|\mathbf{z}_{1:k-1}) = \int p(\mathbf{x}_k^t|\mathbf{x}_{k-1}^t) p(\mathbf{x}_{k-1}^t|\mathbf{z}_{1:k-1})\, d\mathbf{x}_{k-1}^t \tag{1}$$

where $p(\mathbf{x}_k^t|\mathbf{x}_{k-1}^t)$ is a probabilistic Markov motion or process model which maps the probability of transition from a given previous state $\mathbf{x}_{k-1}^t$ to a destination state $\mathbf{x}_k^t$ at time k. The process model is a function of the equations of motion for the target and of the known distribution on their inputs, as well as the environmental constraints impeding the target motion, e.g walls and partitions. Various examples of process models with constraints can be found in [2].

Update At time step k, a new set of observations $\mathbf{z}_k = \{\mathbf{z}_k^1, ..., \mathbf{z}_k^{N_s}\}$ becomes available. For each sensor i, the mapping of the target state observation probability, $\mathbf{z}^i \in \mathbb{R}^{n_z}$, for each given target state, $\mathbf{x}_k^t \in \mathbb{R}^{n_x}$, is denoted $p(\mathbf{z}_k^i|\mathbf{x}_k^t)$ and will be referred to as the observation likelihood, or sensor model. Assuming all the observations to be conditionally independent, the PDF update from the prediction stage (1), $p(\mathbf{x}_k^t|\mathbf{z}_{1:k-1})$, is performed using the following Bayes rule with the normalization coefficient K, also referred to in the literature as the "independent opinion pool"

$$p(\mathbf{x}_k^t|\mathbf{z}_{1:k}) = K\, p(\mathbf{x}_k^t|\mathbf{z}_{1:k-1}) \prod_{i=1}^{N_s} p(\mathbf{z}_k^i|\mathbf{x}_k^t) \tag{2}$$

2.2 Decentralized Coordinated Control

Each of the N_s sensor/vehicle system is governed by its own dynamic model in the form

$$\mathbf{x}_{k+1}^{s_i} = \mathbf{f}_k^{s_i}(\mathbf{x}_k^{s_i}, \mathbf{u}_k^{s_i}, \mathbf{w}_k^{s_i}) \tag{3}$$

where $\mathbf{w}_k^{s_i}$ is the vector representing the process noise and the external forces acting on the system i, and where $\mathbf{u}_k^{s_i}$ is the corresponding control input vector at time k. The controller objective is to produce a command that will place the system in a desired state.

For multiple sensor platforms, an optimal cooperative control solution must be the group decision that is jointly optimal. In decentralized systems, optimal plans are usually intractable and can only be obtained through extensive negotiations between a small number of agents. A solution is to follow a decentralized coordinated control strategy which consists in implementing an independent control law for each sensor. The individual utility function for the i^{th} sensor is denoted $J_k^{s_i}(\mathbf{u}^{s_i}, N_k)$, where $\mathbf{u}^{s_i} = \{\mathbf{u}_1^{s_i}, ...\mathbf{u}_{N_k}^{s_i}\}$ is the control action sequence over a time horizon of length $T = N_k\, \delta t$, where N_k is the number of lookahead steps. The locally optimal control policy $\mathbf{u}^{s_i *}$ is the sequence that maximizes that utility subject to the control bounds $\mathbf{u}_{LB}^{s_i} \leq \mathbf{u}^{s_i} \leq \mathbf{u}_{UB}^{s_i}$ and the constraints $\mathbf{g}^{s_i}(\mathbf{u}^{s_i}, N_k) \leq \mathbf{0}$.

$$\mathbf{u}^{s_i *} = \{\mathbf{u}_1^{s_i *}, ..., \mathbf{u}_{N_k}^{s_i *}\} = \arg\max_{\mathbf{u}^{s_i}} J_k^{s_i}(\mathbf{u}^{s_i}, N_k) \tag{4}$$

The simplest form of coordinated control is implemented with a lookahead depth of one-step corresponding to maximizing N_s independent control laws in the form $J_k^{s_i}(\mathbf{u}_k^{s_i}, 1)$. There is no mechanism to reach a negotiated outcome. Each sensor node exchange information via the network ensuring that each platform builds an equivalent representation of the world, i.e. target state PDF. Coordination results from the platforms affecting each other's local control decisions by contributing to the prior on which these local decisions are made [3,9]. Coordinated trajectories are suboptimal, but they have the appealing advantages of being completely decentralized, computationally very cheap and highly scalable as the nodal planning computation costs do not increase with the number of platforms.

2.3 Active Bayesian Sensor Network

Packaging a physical sensor with its own Bayesian filtering processor is an attractive way of making the sensor mobile and modular. Fig. 1 depicts algorithmically the nodal Bayesian filter and how it interacts with the Controller, the Platform, and the Sensor in a network with node-to-node communication. The Platform block represents the actuators and dynamics of both the sensor and the mobile vehicle, if

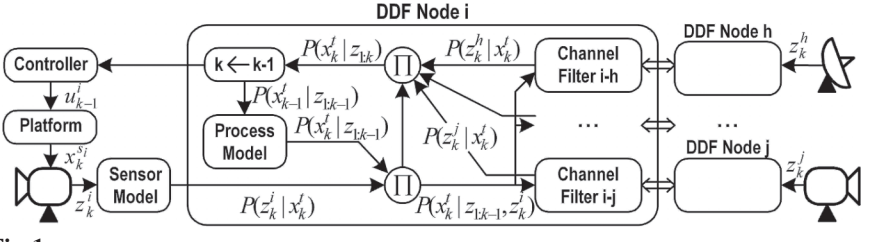

Fig. 1. General active Bayesian sensor node with channel filters for node-to-node communication.

present, on which the sensor is mounted. Based on the latest belief about the world $p(\mathbf{x}_{k-1}^t|\mathbf{z}_{1:k-1})$ and the sensor state $\mathbf{x}_{k-1}^{s_i}$, the Controller sends a command $\mathbf{u}_{k-1}^{s_i}$ to the Platform to place the sensor in a desired position $\mathbf{x}_{k_{des}}^{s_i}$ with respect to the world to take the next observation. When it comes in, the new observation likelihood $p(\mathbf{z}_k^i|\mathbf{x}_k^t)$ is fused with the predicted estimate $p(\mathbf{x}_k^t|\mathbf{z}_{1:k-1})$ to form the new nodal estimate based on an incomplete set of observations $p(\mathbf{x}_k^t|\mathbf{z}_{1:k-1}, \mathbf{z}_k^i) = p(\mathbf{x}_k^t|\mathbf{z}_{1:k}^{*i})$. This latest estimate is then sent to a neighboring node via a Channel Filter whose purpose is to maintain a density estimate based on the common information shared between the two nodes. In order to prevent double-counting, the Channel Filter uses its estimate to remove the common information from the nodal estimate. The residual which corresponds to the new information accumulated by the emitting node, through sensor observations and communication with other neighbors, is then communicated to the Channel Filter of the receiving node to update both the nodal and channel estimates. Likewise, the emitting node also fuses to its estimate prior to communication, $p(\mathbf{x}_k^t|\mathbf{z}_{1:k}^{*i})$, the information that it receives from its neighbors.

If the node is the hub of the network, its new post-communication estimate corresponds to the global estimate based on complete information, $p(\mathbf{x}_k^t|\mathbf{z}_{1:k})$. In general, the nodal density estimate at any given time is based on an incomplete set of observations caused by the time delay necessary for new information to propagate through the network. The discrepancies between the nodal estimates increase with the number of prediction steps and/or observations made between each communication step, as well as the length of the communication chains in the network. However, the channel filter guarantees the nodes to converge to the global estimate given the network propagation delay. The details of the general channel filter are introduced in [1] where it is also proposed to evaluate the amount of estimation error using the following Hellinger affinity measure

$$D(p_i\|p_j) = 2\ln \int \sqrt{p_i(\mathbf{x}_k^t)p_j(\mathbf{x}_k^t)}\, d\mathbf{x}_k^t \tag{5}$$

which is a monotonic distance metric between two densities p_i and p_j [10]. The metric values range from 0, when the densitites are identical, to $-\infty$, when they have nothing in common, i.e. $\int \sqrt{p_i(\mathbf{x}_k^t)p_j(\mathbf{x}_k^t)}\, d\mathbf{x}_k^t = 0$. The channel manager also uses this divergence measure to determine when to communicate on each channel [1]. One necessary condition to maintain proper accounting of the information is that the network connectivity must be acyclic [8]. In other words, no communication loops must exist between the nodes that would enable the information to cycle through multiple times.

3 The Search Problem

This section describes the equations for computing the probability of detection of a lost object referred to as the target by using the outputs of the prediction and update equations from Sec. 2.1. An equivalent but different derivation is presented in [3]. Further details on the searching problem can also be found in [13] and [12] (Chap.9).

Let the target detection likelihood (observation model) of the i^{th} sensor at time step k be given by $p(\mathbf{z}_k^i = D_k^i|\mathbf{x}_k^t)$ where D_k^i represents a 'detection' event by sensor i at time k. The likelihood of 'no detection' by the same sensor is given by its

complement $p(\overline{D}_k^i|\mathbf{x}_k^t) = 1 - p(D_k^i|\mathbf{x}_k^t)$. The combined 'no detection' likelihood for all the sensors at time step k is simply a multiplication of the individual 'no detection' likelihoods

$$p(\overline{D}_k|\mathbf{x}_k^t) = \prod_{i=1}^{N_s} p(\overline{D}_k^i|\mathbf{x}_k^t) \tag{6}$$

where $\overline{D}_k = \overline{D}_k^1 \cap ... \cap \overline{D}_k^{N_s}$ represents the event of a 'no detection' observation by every sensor at time step k. Neglecting the normalization factor K in the update equation (2) gives

$$p(\mathbf{x}_k^t|\mathbf{z}_{1:k})' = p(\mathbf{x}_k^t|\mathbf{z}_{1:k-1})' \prod_{i=1}^{N_s} p(\mathbf{z}_k^i|\mathbf{x}_k^t) \tag{7}$$

The advantage of not normalizing the target PDF at every update is that the joint probability of failing to detect the target in all of the steps from 1 to k, denoted $Q_k = p(\overline{D}_{1:k})$, can be directly obtained from the integration of the pseudo PDF update (7)

$$Q_k = \int p(\mathbf{x}_k^t|\overline{D}_{1:k})' d\mathbf{x}_k^t = \int p(\mathbf{x}_k^t|\overline{D}_{1:k-1})' p(\overline{D}_k|\mathbf{x}_k^t)\, d\mathbf{x}_k^t \tag{8}$$

where $\overline{D}_{1:k}$ corresponds to the set of observations $\mathbf{z}_{1:k}$ where every observation is a 'no detection', i.e. $\mathbf{z}_k = \overline{D}_k, \forall k$. Then, it can be shown that the probability the target gets detected for the first time on time step k, denoted p_k, is given by the volume under the surface resulting from the product of the combined detection likelihood, denoted $\left[1 - p(\overline{D}_k|\mathbf{x}_k^t)\right] = p(D_k|\mathbf{x}_k^t)$, with the predicted target PDF. This is equivalent to the reduction in volume ($-\Delta Q_k$) of the pseudo PDF as in

$$p_k = \int p(\mathbf{x}_k^t|\overline{D}_{1:k-1})' \left[1 - p(\overline{D}_k|\mathbf{x}_k^t)\right] d\mathbf{x}_k^t = Q_{k-1} - Q_k \tag{9}$$

Assuming no false detection from the sensors, the probability that the target *has* been detected in k steps, denoted P_k, is obtained from the cumulative sum of the p_k's as in

$$P_k = \sum_{i=1}^{k} p_i = P_{k-1} + p_k \tag{10}$$

For this reason P_k will be referred to as the 'cumulative' probability of detection to distinguish it from the payoff probability of detection function p_k. Notice that plugging the expressions for p_k from (9) into (10) gives $P_k = 1 - Q_k$ since $Q_0 = \int p(\mathbf{x}_0^t) d\mathbf{x}_0^t = 1$. This signifies that if the target PDF is not normalized after each update as in (7), then its volume, Q_k, represents the residual probability that the target is still present despite the search effort expended. Also, as k goes to infinity, Q_k decreases towards zero and P_k levels off towards one as it becomes harder to generate additional observation payoff, p_k, from hardly any probability mass left in the PDF.

The goal of a searching strategy could be to maximize the chances of finding the target given a restricted amount of time by maximizing P_k over a given time horizon [4]. For a time horizon of one as discussed in Sec. 2.2, the individual utility function reduces to the probability of detecting the target on the next time step, as in

$$J_k^{s_i}(\mathbf{u}_k^{s_i}, 1) = p_k^{s_i} = \int p(\mathbf{x}_k^t|\overline{D}_{1:k-1})' p(D_k^i|\mathbf{x}_k^t)\, d\mathbf{x}_k^t \tag{11}$$

which corresponds to the volume under the surface resulting from the product of the 'detection' likelihood from sensor i with the predicted pseudo target PDF.

4 Experiment

The goal of the ongoing research effort is to demonstrate the effectiveness of the coordinated decentralized search framework on a team of heterogeneous autonomous mobile platforms in real outdoor scenarios. A stepping stone towards this goal is to investigate the problem using simple physical robots in an indoor environment. The remainder of this section presents the implementation details and the results of the decentralized coordinated search framework implemented for a team of three Pioneer 2 robots, each equipped with a laser scanner (Fig. 2a), searching for a single mobile human target throughout the office space of the Australian Centre for Field Robotics (ACFR).

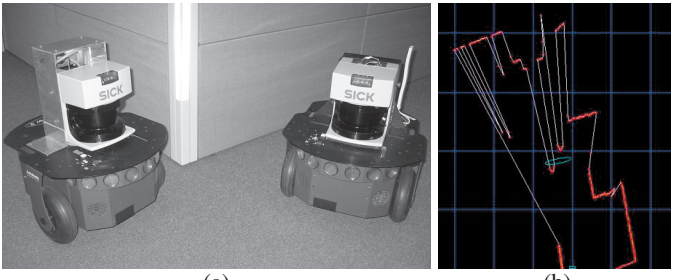

(a) (b)

Fig. 2. Experiment: (a) two of the three Pioneer robots equipped with laser range finders and wireless communication; (b) raw laser scan in which two legs can be distinguished and where the cyan ellipse represents the estimate of the human target location.

4.1 Implementation

The necessary decentralized network components, i.e. controller, platform, sensor and fusion node, were derived from basic C++ classes developed at ACFR as part of the ASN research thrust [11]. The Pioneer platforms are controlled via a publicly available hardware abstraction layer called Player[1]. Prior to the search experiment, the indoor environment (Fig. 4a) was explored to produce an occupancy grid (OG) map of the area (appox. 16x14m), as well as a localization feature map (Fig. 4b) using the SLAM algorithm [6] . The features are stripes of reflective material, as seen on Fig. 2a, returning high laser intensities. Once the SLAM map was judged to be accurate enough, it was stored and subsequently used as a beacon map for localization during the search experiment. The human target motion is modelled *a priori* as a zero mean Gaussian diffusion process, i.e. random walk, with a standard deviation in x and y of 0.35 m/s. The OG map is then used to constrain the resulting tabulated probability of transition $p(\mathbf{x}_k^t|\mathbf{x}_{k-1}^t)$ as in [2]. As for the prior PDF in an indoor environment (Fig. 4b), it could come straight from the estimate of a surveillance system after it lost track of its target. Another possibility could be to use data accumulated over an extended period to produce a prior reflecting the target's preferred location in the environment.

[1] Player was developed jointly at USC Robotics Research Lab. and HRL Labs. and is available under the GNU General Public License from http://playerstage.sourceforge.net

Platform Model Each vehicle i is moving in the xy plane at constant velocity $V_i = .15$ m/s where the single control parameter $u_k^{s_i}$ is the heading rate and is maintained over the time interval δt. In this experiment the maximum heading rate amplitude is set to $u_{max} = \pm 20$ deg/s). The vehicle pose prediction model used for the planning purposes is the following discrete time non-linear constant velocity model

$$x_{k+1}^{s_i} = x_k^{s_i} + \frac{2V_i}{u_k^{s_i}} \sin(\frac{1}{2} u_k^{s_i}\, \delta t) \cos(\theta_k^{s_i} + \frac{1}{2} u_k^{s_i}\, \delta t) \tag{12}$$

$$y_{k+1}^{s_i} = y_k^{s_i} + \frac{2V_i}{u_k^{s_i}} \sin(\frac{1}{2} u_k^{s_i}\, \delta t) \sin(\theta_k^{s_i} + \frac{1}{2} u_k^{s_i}\, \delta t) \tag{13}$$

$$\theta_{k+1}^{s_i} = \theta_k^{s_i} + u_k^{s_i}\, \delta t \tag{14}$$

Observation Model The search sensor is the same laser range finder that is used for navigation. Mounted on top of the Pioneer, its horizontal sensing plane is about mid-distance between the knees and ankles of an adult. This makes it quite an interesting sensor for this experiment as a pair of legs at this height represents a fairly distinct feature that is easy to discriminate [5]. A leg, as sensed by the laser scanner, is modelled as a semi-circle with radius in a certain bounded range, separated from its background by a threshold distance determined experimentally. A human is defined as a pair of legs within a certain distance of each other. Fig. 2b shows the detection of a pair of likely legs in a laser scan.

Fig. 3b illustrates the detection likelihood with respect to the target distance from the sensor. Notice that to make the experiment less trivial, the detection range was artificially reduce from 10 m to 2 m in order to make the limited search area appears relatively larger. As seen on Fig. 3a, the laser scan goes from -90 to +90 degrees with respect to the robot orientation and the resulting detection likelihood, $p(D_k^i|\mathbf{x}_k^t)$, is illustrated on Fig. 3c. If no obstacles are in the sensor range, this is the detection likelihood that enters the utility function (11) to determine the next control action. When a new scan comes in, it is first process to detect the presence of a human. If no contact is made, then the nodal estimate is updated with the 'no detection' likelihood given by $p(\overline{D}_k^i|\mathbf{x}_k^t) = 1 - p(D_k^i|\mathbf{x}_k^t)$.

On a practical note, to ensure proper convergence of the control optimization algorithm, it is important that the detection likelihood be smooth and that it decreases progressively to zero with increasing range and/or bearing without any steps in the function as seen on Fig. 3.

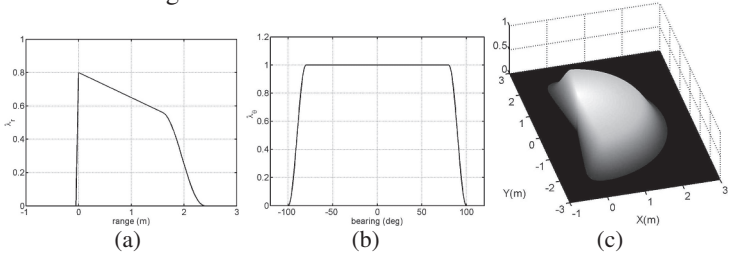

(a) (b) (c)

Fig. 3. Observation Model: (a) detection likelihood vs. range; (b) detection likelihood vs. bearing; (c) 3D view of the detection likelihood over range and bearing, $p(D_k^i|\mathbf{x}_k^t)$, for $\mathbf{x}_k^{s_i} = [0, 0, 0]$.

4.2 Results

Fig. 4 illustrates the decentralized search results for the active Bayesian sensor network algorithm presented in Sec. 2. The robots, namely Hornet, Mozzy and Dragonfly are travelling at constant velocity except when slowing down near obstacles. A modified version of the vector field histogram (VFH) technique [14] ensures that collisions are avoided. One observation and one control decision is made at approximately one second intervals on board each robot. The channel manager communication threshold is set to $D_{thresh} = -.01$. Figs. 4c to f represent snapshots of the evolution of the PDF estimate computed onboard Hornet's node, which is the hub of the network, and the coordinated robot trajectories given the prior density shown on Fig. 4b. Fig. 4g compares the nodal cumulative probability of detection functions $P_k^{s_i}$'s. Fig. 4h is a zoom in of the later and Fig. 4i displays the corresponding divergence evolutions representing the discrepancies between the nodal estimates and the channel estimates over time.

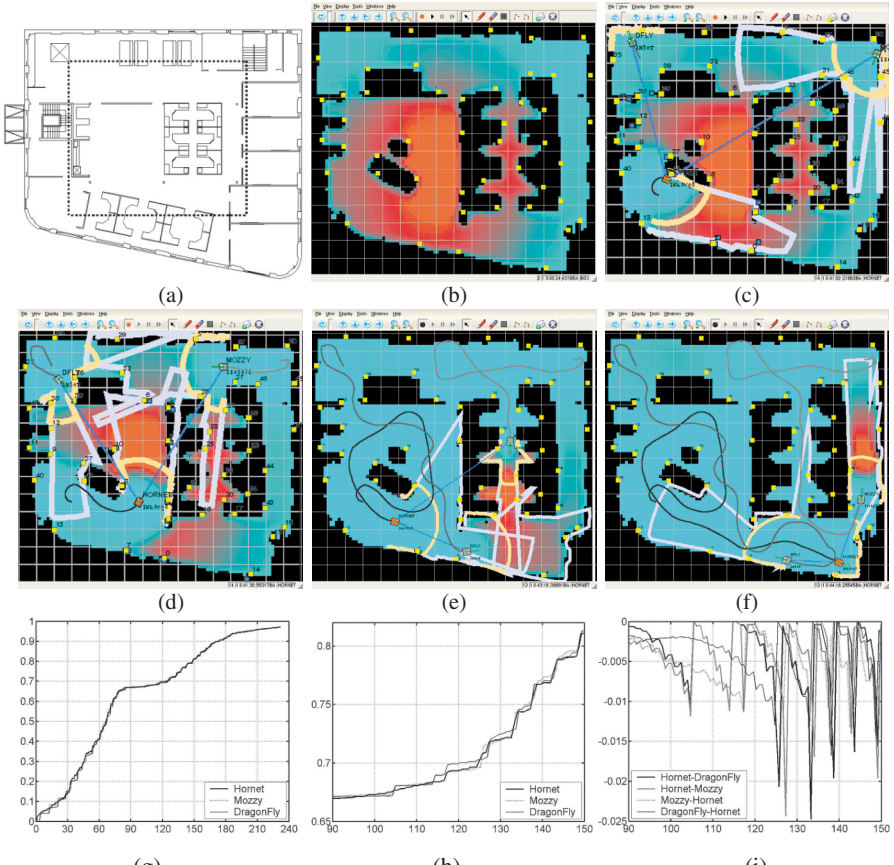

Fig. 4. Coordinated search results with managed node-to-node communication ($D_{thresh} = -.01$): (a) floor plan of ACFR with the 16x14m search area delimited by the dashed line; (b) OG map (black obstacles) and beacon map (small yellow squares) overlaid with the prior target PDF (red equals high density); (c)-(f) snapshots of the target PDF estimate onboard Hornet, the coordinated robot trajectories at 12, 40, 148 and 208 seconds into the search respectively and the network links between the robots (blue lines); (g) cumulative probability of detection P_k vs. time [s]; (h) zoom in of P_k, and (i) the corresponding Hellinger divergence evaluated between the node and channel estimates.

The nodal channel manager uses the divergence measure to adaptively determine when to communicate on any particular channel. The smaller the communication threshold, the more often the nodes communicate and the more accurate their estimates are. This is important as the search platforms are then much less likely to interfere with each other when their density estimates are almost identical. The communication divergence threshold is therefore a compromise between accuracy and bandwidth capacity. Clearly seen on the divergence plot is the synchronization between the nodal and channel estimates occurring at each communication burst. The communication steps can also be easily identified from the steps in the $P_k^{s_i}$ estimates. Also worth noticing on the zoom in of the P_k plot is that once a node communicates, it is usually followed soon after by the receiving nodes which transmit to their other neighbors and so forth until the new information that triggered the chain reaction is propagated throughout the network.

Finally, the efficiency of the coordinated control strategy in allocating the search effort is demonstrated by a final cumulative probability of detection as high as 97.1% for 231s of search. Recall that this performance is reached without the robots exchanging any information about their plans. As mentioned in Sec. 2.2, coordination results from the platforms affecting each other's control decisions by contributing the prior on which these local decisions are made. This is explained by the fact that the utility for a robot to search a region is decreased if another agent is already searching that region. This has the effect of increasing the relative utility of other regions of the space and diverting the former robots towards these regions. In some occasions however, because of the myopic nature of this kind of planning, the robots can fail to detect higher utility regions outside their predicted sensor range and might get stuck circling inside a room instead of getting out and visiting another room with higher payoff values. For these cases, it would be beneficial to implement the control with a time-horizon of adaptive length.

5 Conclusion and Further Work

This paper addressed the implementation issues related to the problem of coordinating multiple, possibly heterogeneous, sensing platforms performing a search mission for a single target in a dynamic environment. The general decentralized Bayesian framework presented constitutes a building block of the much broader problem of management in decentralized systems. It was demonstrated to adaptively find efficient coordinated search plans that explicitly considers the search vehicles kinematics, the sensors detection function, as well as the target arbitrary motion model. Decentralized coordinated solutions, while being suboptimal, are adaptive and offer tremendous scalability potential as their nodal computational costs are kept constant with the number of platforms. The general decentralized Bayesian filtering algorithm was demonstrated to be robust to communication failures and ensured that complete global information was recovered at each node despite delayed communications in the network.

As part of the ongoing research effort, techniques to facilitate human interactions with the active sensor network are being investigated to enable an operator to enter observations in the network and influence the agents control decisions. A novel

approach to cooperative control based on a decentralized negotiation filter that will increase the time horizon of the decentralized search plans is also being developed.

Acknowledgement

This work is partly supported by the ARC Centre of Excellence programme, funded by the Australian Research Council (ARC) and the New South Wales State Government, and by AFOSR/AOARD under contract 03-13.

References

1. F. Bourgault and H.F. Durrant-Whyte. Communication in general decentralized filters and the coordinated search strategy. In *The 7th Int. Conf. on Information Fusion*, Stockholm, Sweden, June 2004.
2. F. Bourgault and H.F. Durrant-Whyte. Process model, constraints, and the coordinated search strategy. In *IEEE Int. Conf. on Robotics and Automation (ICRA'04)*, New Orleans, USA, April 2004.
3. F. Bourgault, T. Furukawa, and H.F. Durrant-Whyte. Coordinated decentralized search for a lost target in a Bayesian world. In *IEEE/RSJ Int. Conf. on Intelligent Robots and Systems (IROS'03)*, October 2003.
4. F. Bourgault, T. Furukawa, and H.F. Durrant-Whyte. Optimal search for a lost target in a Bayesian world. In *Int. Conf. on Field and Service Robotics (FSR'03)*, Japan, July 2003.
5. A. Brooks and S. Williams. Tracking people with networks of heterogeneous sensors. In *Australasian Conf. on Robotics and Automation (ACRA'03)*, Brisbane, Australia, December 2003.
6. G. Dissanayake, P. Newman, S. Clark, H.F. Durrant-Whyte, and M. Csobra. A solution to the simultaneous localization and map building (SLAM) problem. *Robotics and Automation*, 17(3):229–241, 2001.
7. M. Flint, M. Polycarpou, and E. Fernandez-Gaucherand. Cooperative control for multiple autonomous uav's searching for targets. In *41st IEEE Conference on Decision and Control*, Las Vegas, USA, December 2002.
8. S. Grime and H.F. Durrant-Whyte. Communication in decentralized systems. *IFAC Control Engineering Practice*, 2(5):849–863, 1994.
9. B. Grocholsky, A. Makarenko, and H. Durrant-Whyte. Information-theoretic coordinated control of multiple sensor platforms. In *IEEE Int. Conf. on Robotics and Automation (ICRA'03)*, 2003.
10. A.O. Hero, B. Ma, O. Michel, and J. Gorman. Alpha-Divergence for Classification, Indexing and Retreival (Revised 2). Technical Report CSPL-328, Communication and Signal Processing Lab., The University of Michigan, 48109-2120, USA, June 2002.
11. A. Makarenko, A. Brooks, S. Williams, H.F. Durrant-Whyte, and B. Grocholsky. A decentralized architecture for active sensor networks. In *IEEE Int. Conf. on Robotics and Automation (ICRA'04)*, New Orleans, USA, April 2004.
12. J.S. Przemieniecki. *Mathematical Methods in Defense Analyses*. AIAA Education Series. American Inst. of Aeronautics and Astronautics, Inc., Washington, DC, 2nd edition, 1994.
13. L.D. Stone. *Theory of Optimal Search*, volume 118 of *Mathematics in Science and Engineering*. Academic Press, New York, 1975.
14. I. Ulrich and J. Borenstein. VFH+: Reliable obstacle avoidance for fast mobile robots. In *IEEE International Conference on Robotics and Automation (ICRA '98)*, pages 1572–1577, 1998.
15. R. Vidal, S. Rashid, C. Sharp, O. Shakernia, J. Kim, and S.S. Sastry. Pursuit-evasion games with unmanned ground and aerial vehicles. In *IEEE Int. Conf. on Robotics and Automation (ICRA'01)*, Seoul, Korea, May 2001.